Applied Physics Letters

Weak localization and dimensional crossover in compositionally graded $Al_xGa_{1-x}N$

Cite as: Appl. Phys. Lett. **118**, 082101 (2021); https://doi.org/10.1063/5.0042098
Submitted: 28 December 2020 . Accepted: 09 February 2021 . Published Online: 24 February 2021

Athby Al-Tawhid, Abdullah-Al Shafe, Pegah Bagheri, Yan Guan, Pramod Reddy, Seiji Mita, Baxter Moody, Ramon Collazo, Zlatko Sitar, and Kaveh Ahadi

Applied Physics Letters ARTICLE scitation.org/journal/apl

Weak localization and dimensional crossover in compositionally graded $Al_xGa_{1-x}N$

Cite as: Appl. Phys. Lett. **118**, 082101 (2021); doi: 10.1063/5.0042098
Submitted: 28 December 2020 · Accepted: 9 February 2021 ·
Published Online: 24 February 2021

Athby Al-Tawhid,[1] Abdullah-Al Shafe,[1] Pegah Bagheri,[1] Yan Guan,[1] Pramod Reddy,[2] Seiji Mita,[2] Baxter Moody,[2] Ramon Collazo,[1] Zlatko Sitar,[1] and Kaveh Ahadi[1,a]

AFFILIATIONS

[1]Department of Materials Science and Engineering, North Carolina State University, Raleigh, North Carolina 27695, USA
[2]Adroit Materials Inc., 2054 Kildaire Farm Road, Suite 205, Cary, North Carolina 27518, USA

[a]Author to whom correspondence should be addressed: kahadi@ncsu.edu

ABSTRACT

The interaction between the itinerant carriers, lattice dynamics, and defects is a problem of long-standing fundamental interest for developing quantum theory of transport. Here, we study this interaction in the compositionally and strain-graded AlGaN heterostructures grown on AlN substrates. The results provide direct evidence that a dimensional crossover (2D–3D) occurs with increasing temperature as the dephasing scattering events reduce the coherence length. These heterostructures show a robust polarization-induced 3D electron gas and a metallic-like behavior down to liquid helium temperature. Using magnetoresistance measurements, we analyze the evolution of the interaction between charge carriers, lattice dynamics, and defects as a function of temperature. A negative longitudinal magnetoresistance emerges at low temperatures, in line with the theory of weak localization. A weak localization fit to near zero-field magneto-conductance indicates a coherence length that is larger than the elastic mean free path and film thickness ($l_\varphi > t > l_{el}$), suggesting a 2D weak localization in a three-dimensional electron gas. Our observations allow for a clear and detailed picture of two distinct localization mechanisms that affect carrier transport at low temperature.

Quantum corrections to the charge transport due to the coherent interference of carriers could provide insight into the fundamental transport phenomena of charge carriers.[1–3] For example, these corrections could shed light on the interactions between the itinerant carriers and lattice dynamics.[4] Weak localization reduces the conductivity below the Drude picture due to the coherent interference of the time-reversed pairs of Feynman paths.[5] The charge carriers return to the point of origin after a series of elastic scattering events, increasing the resistivity. Weak localization could be used to probe defects and their interactions with charge carriers in semiconductors.[6–9]

AlGaN alloys have attracted attention for high-frequency, high-power, and optoelectronic applications.[10] Conventional electron doping of AlGaN becomes limited with the increasing Al concentration, i.e., widening bandgap.[11,12] Furthermore, conventional p-doping of these semiconductors remains elusive. The polarization gradient, however, could induce both electron and hole gases in two- or three-dimensions.[13–15] The conventionally doped semiconductors demonstrate a carrier freeze-out at cryogenic temperatures. The polarization-induced charge carriers, however, are robust and survive down to liquid helium temperature where charge-defect and charge-charge interactions become dominant, providing a unique opportunity to study these interactions in III-nitride semiconductors. Weak localization has been observed in 2D electron systems at the GaN/AlGaN interface.[16] Weak localization becomes pronounced with lowering of dimensionality and is rarely observed in 3D systems.[17] The dimensional crossover in weak localization has not been reported in AlGaN.

Here, we study the weak localization in compositionally and strain-graded AlGaN heterostructures. The polarization gradient, due to a combination of spontaneous polarization, piezoelectricity, and flexoelectricity, induces a robust 3D electron system. We observe weak localization and dimensional crossover in these heterostructures at the low temperature limit. It would also be interesting to probe quantum corrections to conductivity in hole-doped systems.

The compositionally and strain-graded AlGaN heterostructures were grown on single crystalline AlN substrates (HexaTech, Inc.)[18,19] using metal organic chemical vapor deposition (MOCVD). The growth details are described elsewhere.[20] Figure 1(a) shows the schematic cross section of the heterostructure used in this study. 100 nm of unintentionally doped (UID) and compositionally graded $Al_xGa_{1-x}N$ (0.56 to 1) was grown on $Al_{0.56}Ga_{0.44}N$ (200 nm)/AlN (100 nm)/AlN.

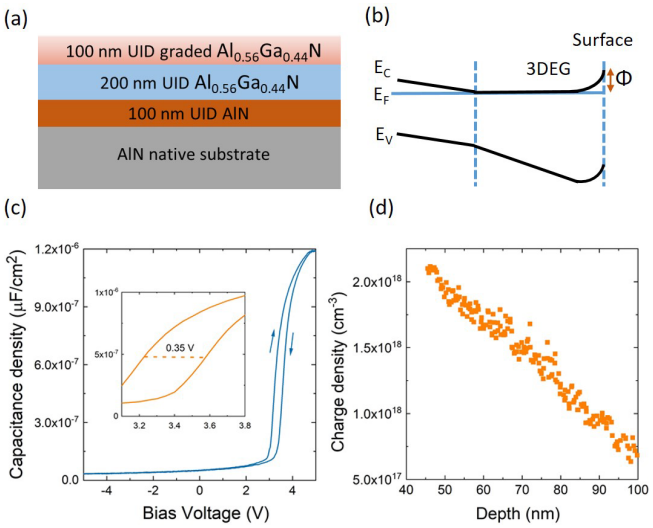

FIG. 1. The compositionally and strain-graded $Al_{1-x}Ga_xN$ heterostructure. The schematic (a) cross section and (b) band structure of the heterostructure. (c) The CV measurements at 10 KHz, resolving (d) the carrier density with the depth.

The aluminum/gallium ratio was determined using a secondary ion mass spectroscopy (SIMS) approach described elsewhere.[21] X-ray diffraction (XRD) was performed to characterize the crystalline quality of the heterostructures using a Philips X'Pert Materials Research Diffractometer system. XRD scans revealed that all heterostructures were epitaxial, single phase, and (0001)-oriented (Supplementary Information, Fig. 1). The 0002 diffraction revealed well-defined crystalline peaks for the AlN and $Al_{0.56}Ga_{0.44}N$ layers, while the compositionally graded film shows a plateau in the diffraction intensity that stretches between the diffraction peaks of the uniform-composition layers. Temperature-dependent Hall and longitudinal resistances were measured using a Quantum Design Physical Property Measurement System. Magnetotransport measurements were carried out in the van der Pauw geometry with square-shaped samples. Ohmic contacts (V(30 nm)/Al(100 nm)/Ni(70 nm)/Au(70 nm)) were deposited on the sample corners through a shadow mask using electron beam evaporation. The contacts were activated using a rapid thermal annealing procedure at 950 °C for 30 s. Capacitance measurements were carried out at room temperature using a Keithley 4200 semiconductor parameter analyzer with circular Ni Schottky contacts (70 μm diameter). A linear fit of A^2/C^2 with applied bias, where A is the contact area and C is the capacitance, revealed an ~2.8 eV Schottky barrier (Supplementary Information, Fig. 2).

The compositional grading induces a spontaneous polarization gradient across the $Al_{1-x}Ga_xN$ layer. In addition, the epitaxial strain and strain gradient induce polarization due to piezoelectric and flexoelectric responses, respectively. The 180° domains typically emerge to screen the large depolarization field in polar thin films.[22,23] The fixed surface polarization charges in polar AlGaN, however, force a single domain structure. In the absence of 180° domains, screening charges are necessary to sustain the finite spatial divergence in polarization $\left(\nabla \cdot \vec{P} = \sigma_b\right)$. Figure 2(b) shows the schematic band structure of the heterostructure with a polarization-induced 3D electron gas formed in the compositionally graded $Al_xGa_{1-x}N$ layer. The surface states pin

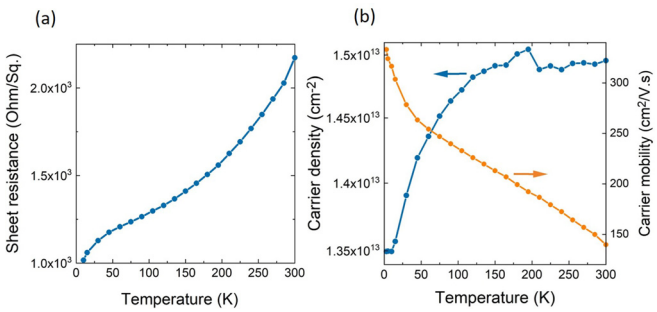

FIG. 2. Charge transport with temperature. (a) Sheet resistance and (b) carrier density and mobility with temperature.

the Fermi level, creating a surface depletion layer shown in Fig. 1(b). Polarization-induced 3D doping has been reported previously in compositionally graded III-nitride thin films.[14]

Figure 1(c) shows the normalized capacitance with bias voltage measured at 10 kHz. The C-V characteristics show a clockwise hysteresis (~0.35 V). The hysteresis is potentially due to the interfacial traps.[24] Figure 1(d) shows the polarization-induced charge density as a function of depth $(N(x) = 2/q\varepsilon m(x)$, where q is the elementary charge, ε is the dielectric constant, and $m(x) = d(A^2/C^2)/dV)$. The charge density distribution across the graded layer confirms the 3D nature of charge carriers. The polarization-induced charge carriers are given by

$$\sigma_b = \nabla \cdot \left(\vec{P}_{SP} + \vec{P}_{PZ} + \vec{P}_{FX}\right),$$

where $\vec{P}_{SP}$, $\vec{P}_{PZ}$, and $\vec{P}_{FX}$ are the spontaneous, piezoelectric, and flexoelectric components of induced polarization, respectively. The variation of charge density with the depth in Fig. 1(d) is potentially due to a combination of surface depletion and nonlinear variation of polarization components. Spontaneous polarization is along the c axis directed to the N-polar face in wurtzite AlGaN. The polarization difference between the polar surfaces of AlN and $Al_{0.56}Ga_{0.44}N$ is $\sim 2.5 \times 10^{-6}$ C cm^{-2}, requiring a screening electron density of 1.6×10^{13} cm^{-2}. The piezoelectric component of polarization is $\sim -1.4 \times 10^{-6}$ C cm^{-2} at the bottom interface and vanishes at the top surface (supplementary material). The flexoelectric polarization response, however, does not show a variation across the film, assuming a linear grading of the lattice constant with the depth. A linear approximation between the spontaneous polarization charge, lattice constant, and Al concentration is obtained.[25] Here, we neglect the flexoelectric component of polarization divergence. The piezoelectric and spontaneous components of polarization divergence have the same sign and require a total screening charge density of 2.5×10^{13} cm^{-2}. The room temperature Hall electron carrier density is 1.5×10^{13} cm^{-2}, close to the predicted value of the polarization-induced charge density. Formation of mobile charge carriers is not the only possible screening mechanism. Charged defects could also screen the induced polarization. For example, formation of vacancy complexes could compensate this polarization gradient. Frequently, a combination of mobile electrons, holes, and charged defects screens the induced polarization divergence. Here, we observe a close match between the predicted and observed values of polarization-induced mobile electron density, suggesting a low concentration of charged defects.

Figure 2(a) shows the sheet resistance of the compositionally graded AlGaN heterostructure measured between 300 and 3 K. The heterostructure shows a metallic-like behavior, $\frac{dR}{dT} > 0$, down to 3 K. The slope of sheet resistance increases below 50 K. Figure 2(b) shows the Hall sheet electron density and mobility between 300 and 3 K. It shows a weak temperature dependence of carrier density, only a $1.5 \times 10^{12}\,\mathrm{cm}^{-2}$ carrier loss in the measured temperature range, revealing a robust 3D electron gas in these heterostructures. The temperature dependence may suggest a weak carrier trapping. It could also be a result of the particular behavior of transverse and longitudinal scattering rates in the polar films, as discussed elsewhere.[26–28] The carrier mobility is $140\,\mathrm{cm}^2/\mathrm{V\,s}$ at room temperature and increases to $333\,\mathrm{cm}^2/\mathrm{V\,s}$ at 3 K. It shows a linear enhancement with temperature between 300 and 50 K. A mobility of $\sim 350\,\mathrm{cm}^2/\mathrm{V\,s}$ was previously reported in the compositionally graded AlGaN (30% Al grading) grown on the GaN substrate at 400 K.[29] The increase in the slope of sheet resistance below 50 K is reflected in the carrier mobility. The room temperature mobility is controlled by the electron-phonon scattering events. Low temperature mobility, however, is dominated by the electron-electron and electron-defect scattering phenomena. The electron-electron interactions are characterized by the Coulomb to Fermi energy ratio ($r_s = \left(\frac{3}{4}\pi n a_0^3\right)^{1/3}$, where n is the carrier density and a_0 is the effective Bohr radius).[30,31] The values below unity indicate weak electron-electron interactions.[30,32] This ratio is 0.26 in this heterostructure, suggesting a weakly interacting system and insignificant electron-electron interactions.

The elastic mean free path, $l_{el} \propto \mu n^{1/2}$, is 17 nm at 3 K, confirming a 3D electronic energy spectrum ($l_{el} < t$). The coherence length (l_φ), however, could diverge in the absence of dephasing scattering events, e.g., electron-phonon scattering, at the absolute zero. Figure 3 shows the longitudinal magnetoresistance at different temperatures. High-temperature magnetoresistance measurements show a quadratic behavior, in line with the classical theory of magnetoresistance in metals.[33] The conductivity change with temperature and magnetic field, ignoring the spin–orbit and Zeeman contributions, is given by

$$\Delta\sigma_{xx}^{T}(B,\,T) = ne\mu\left[\frac{1}{(1+\mu^2B^2)} - 1\right] + \Delta\sigma_{xx}^{WL},$$

where the longitudinal conductivity is obtained from $\sigma_{xx} = \rho_{xx}/[\rho_{xx}^2 + \rho_{xy}^2]$. At lower temperatures (<50 K), a negative magnetoresistance emerges. This behavior has been considered a signature of weak localization. The weak localization occurs when the coherence length becomes larger than the elastic mean free path ($l_\varphi \gg l_{el}$), and as a result, the self-crossing paths could interfere. Electron-phonon and electron-electron scatterings are typically the main dephasing events. Screening of phonons at low temperature and weak electron-electron interactions in this heterostructure enhance the coherence length beyond the elastic mean free path. The applied magnetic field breaks the time reversal symmetry and disrupts the interference of the self-crossing paths, lowering the resistivity.[4,5]

From these experimental results, our main findings are as follows: (i) A robust 3D electron gas is observed in compositionally and strain-graded AlGaN heterostructures due to the polarization gradient, (ii) the carrier density is weakly temperature dependent with a metallic-like behavior ($dR/dT > 0$) down to 3 K, and (iii) signatures of weak localization are observed in the longitudinal magnetoresistance at low temperatures, which grow with decreasing temperature. The sheet resistance, however, does not show resistance upturn below 50 K. The magnitude of weak localization correction from the longitudinal magnetoresistance is ~2.5% at 3 K, which is much smaller than electron mobility enhancement between 50 and 3 K, suggesting an elastic scattering control of the sheet resistance.

The important conclusion from these results is that the magnitude of weak localization enhances with decreasing temperature, suggesting a 2D weak localization. The low temperature 2D weak localization shows a logarithmic correction of conductivity with coherence time, while the 3D weak localization conductivity correction is inversely proportional to the coherence length.[34] Near zero-field 2D weak localization conductance correction is approximated by

$$\Delta\sigma_{xx}^{WL} = \frac{e^2}{h}\frac{2\pi}{3}\left(\frac{l_\varphi^2}{\frac{h}{e}}\right)^2 B^2.$$

While the electronic system is considered to be 3D, the weak localization could become 2D if the coherence length becomes larger than the film thickness at low temperatures.[35] The coherence time declines with increasing temperature, $\tau_\varphi \propto T^{-p}$ for a 2D weak localization, where p depends on the nature of scattering,[17] triggering a *dimensional crossover*. The dimensional crossover affects the nature of weak localization and correction in conductivity. The conductance correction near zero-field, ±50 mT, indicates a coherence length of 127 nm at 3 K. Here, the coherence length is larger than the active layer thickness, suggesting a 2D weak localization at this temperature. The coherence length decreases with increasing temperature and frequency of dephasing events, triggering a dimensional crossover to 3D weak localization. Similar dimensional crossover was previously observed in the 90-nm-thick n-doped GaAs thin films where a dimensional crossover between 2D and 3D weak localizations occurs at 40 K.

In summary, our experimental results, especially the temperature dependence of the observed negative magnetoresistance, should be of

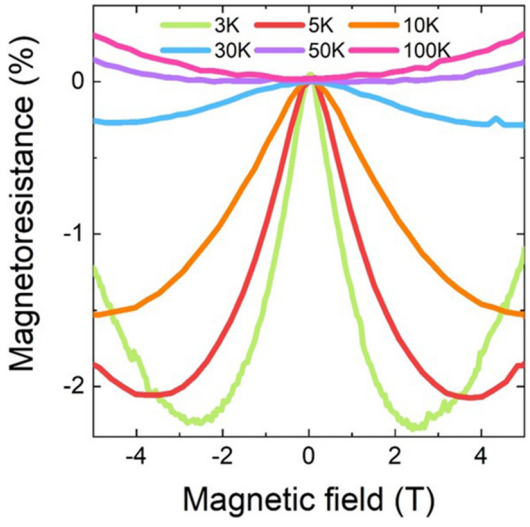

FIG. 3. Weak localization correction in resistance. Longitudinal magnetoresistance with temperature. A negative magnetoresistance emerges at low temperature, indicating a weak localization of charge carriers.

interest for testing the different theoretical models that have been proposed in the literature that relate scattering mechanisms in nitride semiconductors.[36,37] The polarization-induced electrons could survive down to cryogenic temperatures, revealing the electron-defect interaction phenomena and knobs to increase the coherence length of the charge carriers in III-nitride semiconductors. Increasing the coherence length is of importance for the design of the nitride devices ranging from resonant tunneling diode (RTD) oscillators to quantum cascade lasers (QCLs). Finally, it would also be interesting to explore whether similar weak localization and dimensional crossover could be observed in the polarization-induced hole systems in III-nitride semiconductors.

See the supplementary material for XRD data, the Schottky energy barrier height measurement, and the calculation of spontaneous, piezoelectric, and flexoelectric polarization gradient contributions.

Transport measurements were supported by NC State University startup funds. Materials growth was supported in part by AFOSR (Nos. FA9550-17-1-0225 and FA9550-19-1-0114) and NSF (Nos. ECCS-1916800 and ECCS-1653383).

DATA AVAILABILITY

The data that support the findings of this study are available from the corresponding author upon reasonable request.

REFERENCES

[1]D. J. Bishop, R. C. Dynes, and D. C. Tsui, Phys. Rev. B **26**, 773 (1982).
[2]C. W. J. Beenakker, Phys. Rev. B **46**, 12841 (1992).
[3]R. G. Mani, L. Ghenim, and J. B. Choi, Solid State Commun. **79**, 693 (1991).
[4]G. Bergmann, Phys. Rep. **107**, 1 (1984).
[5]S. Chakravarty and A. Schmid, Phys. Rep. **140**, 193 (1986).
[6]F. Rullier-Albenque, H. Alloul, and R. Tourbot, Phys. Rev. Lett. **87**, 157001 (2001).
[7]T. Wang, L. R. Thoutam, A. Prakash, W. Nunn, G. Haugstad, and B. Jalan, Phys. Rev. Mater. **1**, 061601 (2017).
[8]K. Ahadi and S. Stemmer, Phys. Rev. Lett. **118**, 236803 (2017).
[9]K. Ahadi, X. Lu, S. Salmani-Rezaie, P. B. Marshall, J. M. Rondinelli, and S. Stemmer, Phys. Rev. B **99**, 041106 (2019).
[10]J. Y. Tsao, S. Chowdhury, M. A. Hollis, D. Jena, N. M. Johnson, K. A. Jones, R. J. Kaplar, S. Rajan, C. G. Van de Walle, E. Bellotti, C. L. Chua, R. Collazo, M. E. Coltrin, J. A. Cooper, K. R. Evans, S. Graham, T. A. Grotjohn, E. R. Heller, M. Higashiwaki, M. S. Islam, P. W. Juodawlkis, M. A. Khan, A. D. Koehler, J. H. Leach, U. K. Mishra, R. J. Nemanich, R. C. N. Pilawa-Podgurski, J. B. Shealy, Z. Sitar, M. J. Tadjer, A. F. Witulski, M. Wraback, and J. A. Simmons, Adv. Electron. Mater. **4**, 1600501 (2018).
[11]P. Bagheri, R. Kirste, P. Reddy, S. Washiyama, S. Mita, B. Sarkar, R. Collazo, and Z. Sitar, Appl. Phys. Lett. **116**, 222102 (2020).
[12]S. Washiyama, P. Reddy, B. Sarkar, M. H. Breckenridge, Q. Guo, P. Bagheri, A. Klump, R. Kirste, J. Tweedie, S. Mita, Z. Sitar, and R. Collazo, J. Appl. Phys. **127**, 105702 (2020).
[13]R. Chaudhuri, S. J. Bader, Z. Chen, D. A. Muller, H. G. Xing, and D. Jena, Science **365**, 1454 (2019).
[14]Y. Enatsu, C. Gupta, M. Laurent, S. Keller, S. Nakamura, and U. K. Mishra, Appl. Phys. Express **9**, 075502 (2016).
[15]M. A. Khan, J. N. Kuznia, J. M. Van Hove, N. Pan, and J. Carter, Appl. Phys. Lett. **60**, 3027 (1992).
[16]A. F. Braña, C. Diaz-Paniagua, F. Batallan, J. A. Garrido, E. Muñoz, and F. Omnes, J. Appl. Phys. **88**, 932 (2000).
[17]E. Abrahams, P. W. Anderson, D. C. Licciardello, and T. V. Ramakrishnan, Phys. Rev. Lett. **42**, 673 (1979).
[18]P. Lu, R. Collazo, R. Dalmau, G. Durkaya, N. Dietz, B. Raghothamachar, M. Dudley, and Z. Sitar, J. Cryst. Growth **312**, 58 (2009).
[19]D. Zhuang, Z. Herro, R. Schlesser, and Z. Sitar, J. Cryst. Growth **287**, 372 (2006).
[20]R. Dalmau, B. Moody, R. Schlesser, S. Mita, J. Xie, M. Feneberg, B. Neuschl, K. Thonke, R. Collazo, A. Rice, J. Tweedie, and Z. Sitar, J. Electrochem. Soc. **158**, H530 (2011).
[21]C. J. Gu, F. A. Stevie, C. J. Hitzman, Y. N. Saripalli, M. Johnson, and D. P. Griffis, Appl. Surf. Sci. **252**, 7228 (2006).
[22]S. Salmani-Rezaie, K. Ahadi, and S. Stemmer, Nano Lett. **20**, 6542 (2020).
[23]S. Salmani-Rezaie, K. Ahadi, W. M. Strickland, and S. Stemmer, Phys. Rev. Lett. **125**, 087601 (2020).
[24]K. Ahadi and K. Cadien, RSC Adv. **6**, 16301 (2016).
[25]V. Fiorentini, F. Bernardini, and O. Ambacher, Appl. Phys. Lett. **80**, 1204 (2002).
[26]K. Ahadi, L. Galletti, and S. Stemmer, Appl. Phys. Lett. **111**, 172403 (2017).
[27]K. Ahadi, H. Kim, and S. Stemmer, APL Mater. **6**, 056102 (2018).
[28]K. Ahadi, L. Galletti, Y. Li, S. Salmani-Rezaie, W. Wu, and S. Stemmer, Sci. Adv. **5**, eaaw0120 (2019).
[29]J. Simon, A. Wang, H. Xing, S. Rajan, and D. Jena, Appl. Phys. Lett. **88**, 042109 (2006).
[30]S. V. Kravchenko and M. P. Sarachik, Rep. Prog. Phys. **67**, 1 (2004).
[31]A. A. Shashkin, M. Rahimi, S. Anissimova, S. V. Kravchenko, V. T. Dolgopolov, and T. M. Klapwijk, Phys. Rev. Lett. **91**, 046403 (2003).
[32]D. Pines, Rep. Prog. Phys. **79**, 092501 (2016).
[33]A. B. Pippard, *Magnetoresistance in Metals*, 1st ed. (Cambridge University Press, 1989).
[34]B. L. Altshuler, D. Khmel'nitzkii, A. I. Larkin, and P. A. Lee, Phys. Rev. B **22**, 5142 (1980).
[35]A. M. Gilbertson, A. K. M. Newaz, W. J. Chang, R. Bashir, S. A. Solin, and L. F. Cohen, Appl. Phys. Lett. **95**, 012113 (2009).
[36]A. Srivastava, A. Saxena, P. K. Saxena, F. K. Gupta, P. Shakya, P. Srivastava, M. Dixit, S. Gambhir, R. K. Shukla, and A. Srivastava, Sci. Rep. **10**, 18706 (2020).
[37]A. Konar, T. Fang, N. Sun, and D. Jena, Appl. Phys. Lett. **98**, 022109 (2011).